

Figure 1. Deposition process of TS-1 zeolites on stainless steel packing rings.

tetrapropylammonium hydroxide (17 wt %) were used in the synthesis of the zeolites. Hydrogen peroxide (H_2O_2 , 30%), styrene (98%), and acetone (99.5%) for the reaction study and the ethanol (99.7%) and isopropyl alcohol (IPA, 99.7%) solvents were purchased from Tianjin Kernel Chemical Reagents Ltd. Co. Nitric acid (65–68%) and 3-aminopropyltrimethoxysilane (APTS, 98%) were supplied by Dandong Reagents Co and Jiangnan Fine Chemical Co, respectively.

2.2. Preparation of TS-1 Films on Stainless Steel Packing Rings. Seeding is a critical part of many thin film coating and deposition processes.^{31–34} The schematic drawing in Figure 1 illustrates the procedure for the assembly of silicalite-1 (Sil-1) seeds and deposition of TS-1 films on the surface of stainless steel packing rings. The stainless steel packing rings were first degreased by successive 10 min sonication in 0.5 M nitric acid solution, acetone, and ethanol before a thorough rinsing in distilled water. After drying in an oven at 373 K, the packing rings were seeded with 200 nm Sil-1 seeds prepared by hydrothermal synthesis from a synthesis gel with a molar composition of 1 $\text{SiO}_2/0.22 \text{ TPA}_2\text{O}/19.2 \text{ H}_2\text{O}$ for 8 h at 398 K.^{16,35} The seeds were recovered and purified by a series of centrifugation and washing steps before dilution to give a colloidal sol of 0.07 wt % Sil-1 seeds in ethanol. The seeding proceeds by first grafting an organic linker, APTS, on the stainless steel surface, followed by the deposition of a layer of Sil-1 seeds. This was accomplished by immersing the treated packing rings in an autoclave containing the seeds at 373 K for 4 h as described in our prior work.³⁶ The seeded packing rings were dried in an oven at 373 K and calcined at 523 K for 6 h.

The titanium silicalite-1 was deposited and grown on the surface of the seeded packing rings from a clear synthesis solution with a molar composition of 1 $\text{SiO}_2/0.02 \text{ TiO}_2/0.16 \text{ TPA}_2\text{O}/250 \text{ H}_2\text{O}$ under hydrothermal conditions at a temperature of 448 K.¹⁶ The reaction was quenched by rapid cooling, and the zeolite-coated packing rings were rinsed with ethanol and water and dried overnight in an oven at 333 K, followed by calcinations in air or pyrolysis in nitrogen at 823 K for 6 h at a heating rate of $0.3 \text{ K}\cdot\text{min}^{-1}$. The pyrolyzed catalysts were also heat-treated in air at a lower temperature. The pretreatment served to remove the organic template molecules from the zeolites and convert the zeolite coating into an active catalyst.

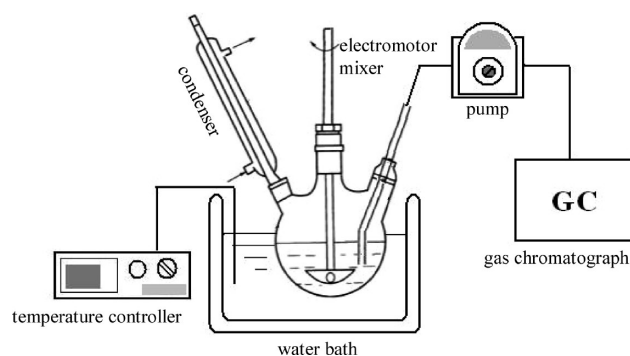


Figure 2. Schematic drawing of the reaction setup.

2.3. Catalyst Characterizations and Activity Test. The zeolite-coated samples were examined by scanning electron microscope (SEM, KYKY-2800B and JEOL 6700F) and characterized by a D/Max 2400 Rigaku X-ray diffractometer equipped with Cu $\text{K}\alpha$ radiation source ($\lambda = 0.1542 \text{ nm}$) and operated at a voltage of 40 kV and 50 mA to determine the thickness, microstructure, crystallinity, and phase composition of the deposited zeolite. The chemical composition was analyzed by energy dispersive X-ray (EDX) and XPS. The bulk compositions of TS-1 powders collected from the bottom of the synthesis batch were determined by X-ray fluorescence spectroscopy (XRF, SRS3400). The samples were analyzed by a Bruker EQUINOX55 Fourier transformed infrared spectrometer and Jasco V-550 UV–vis spectrometer.

The oxidation of styrene to phenylacetaldehyde and benzaldehyde was carried out in the laboratory batch reactor shown in Figure 2. The main product and byproduct of the reaction were phenylacetaldehyde (PAC) and benzaldehyde (BAL), respectively. Mixing was done using a multiblade impeller, and in a typical reaction, the catalyst and 2.1 mL hydrogen peroxide aqueous solution were added to a solution of 9.4 mL of styrene in 27.8 mL acetone to give a reaction mixture of molar composition of 1 styrene/ $0.3 \text{ H}_2\text{O}_2/1.5 \text{ H}_2\text{O}/4.6 \text{ CH}_3\text{COCH}_3$. The reaction was run at 343 K and lasted 5 h. Samples were withdrawn using a pump and analyzed by a gas chromatograph (GC7890F, Shanghai Techcomp Limited) equipped with a flame ionization detector.

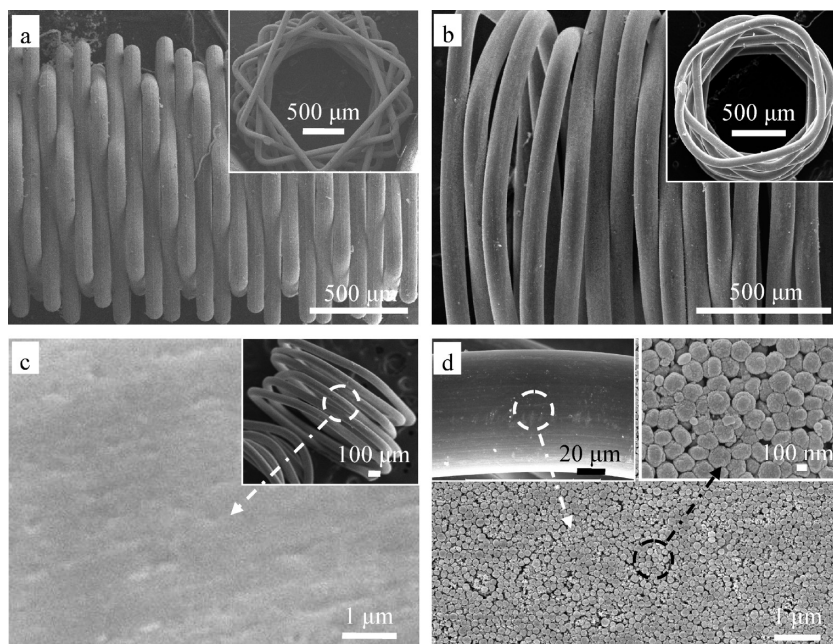


Figure 3. (a, b) SEM images of the stainless steel packing rings, (c) surface of the stainless steel rings, and (d) seeded stainless steel rings support.

A SE-30 capillary column ($150\text{ m} \times \Phi 0.32\text{ mm} \times 0.5\text{ }\mu\text{m}$) was used, and the styrene conversion, product selectivity, and yield were reported.¹⁵

3. RESULTS AND DISCUSSION

3.1. Seeding and Coating of Stainless Steel Packing Rings.

Figure 3a, b is scanning electron micrographs of the stainless steel packing rings before seeding and zeolite coating. It can be seen from the micrographs that the packing rings were made by winding $100\text{-}\mu\text{m}$ -diameter wires into the ordered and random cylindrical coils (Figure 3a and b). Analysis by the energy-dispersive X-ray spectrometer indicated that the wires contained 67.7 wt % iron, 16.7 wt % chromium, and 8.3 wt % nickel. From Figure 3c, it can be seen that the surface of stainless steel packing rings was smooth. Attempts to deposit and grow zeolites on the smooth wire surface by direct synthesis method were unsuccessful due to the poor adhesions of the nucleated zeolite seeds. Seeding eliminated unwanted contributions from the support and could be used to regulate the growth and microstructure of the deposited zeolite.^{37–39} It was not possible to obtain a continuous seed layer on the smooth wire surface by conventional dip-coating and slip-coating methods, and the uneven coating resulted in poor zeolite deposition.

The seeds were assembled on the surface of the wires forming the packing rings using organic linkers. It can be seen in Figure 3d that despite the complex geometry, a uniform layer of seeds was deposited using this technique. The seeds were covalently attached to the $-\text{Si}(\text{OR})_3$ group of the APTS molecule and linked by the amino head groups (Lewis base) to the stainless steel surface (Lewis acid). Conducting the seeding at 373 K ensured the complete condensation and firm attachment of the Sil-1 seeds to the stainless steel surface.³⁶ SEM examination indicated that a monolayer of close-packed Sil-1 seeds was obtained over the entire surface of the packing ring, as shown in the Figure 3d insert.

Titanium silicalite-1 zeolite was grown on the seeded stainless steel packing rings by hydrothermal regrowth from a dilute synthesis solution containing titanium precursor. Prior works showed that it was not necessary to employ TS-1 seeds to deposit and grow TS-1 films on surfaces, and seeds of Sil-1 isomorph were easier to prepare with consistent size and composition.^{15,16} Figure 4 displays the SEM micrographs of the zeolite-coated stainless steel packing rings following heat treatment in air (CP1) and nitrogen (CP2) to remove the organic template molecules. The TS-1 grown on the seeded support formed a continuous layer of a well-intergrown, polycrystalline film of uniform $4\text{-}\mu\text{m}$ thickness over the entire surface of the packing rings. The zeolite growth extends through the seed layer to the surface, forming a single polycrystalline film (Figure 4b inset).

Figure 4a, b shows that high temperature pyrolysis in nitrogen prevented the cracks and delamination of zeolite that were prevalent in samples calcined in air (Figure 4c, d) under a similar temperature program. This is due in part to the large stress generated when the zeolite lattice contracts with the rapid removal and gasification of the trapped organic templates during calcinations. Pyrolysis slowed the gasification of the organic SDA and prevented formation of defects. Similar slow gasification can be achieved using low-temperature ozonidation in preparing low-defect zeolite membranes.^{40–42} Slow heating and cooling rates were necessary precautions to minimize the effects of a large difference in the thermal expansion coefficients of the stainless steel and zeolite.

Fejes et al.⁴³ reported that heat treatment of Ti-substituted ZSM-5 zeolite results in a loss of framework titanium with accompanying lattice shrinkage and a blue shift in IR spectra. Table 1 shows nitrogen pyrolysis preserves the framework titanium in the TS-1 film. The table shows the framework titanium is significantly lower for the TS-1 prepared by air calcination. The X-ray diffractions of the stainless steel packing rings before and after zeolite coating are shown in Figure 5a, b along with the zeolite powder collected from the bottom of the synthesis batch (Figure 5c). The TS-1 film (CP2) grown on the

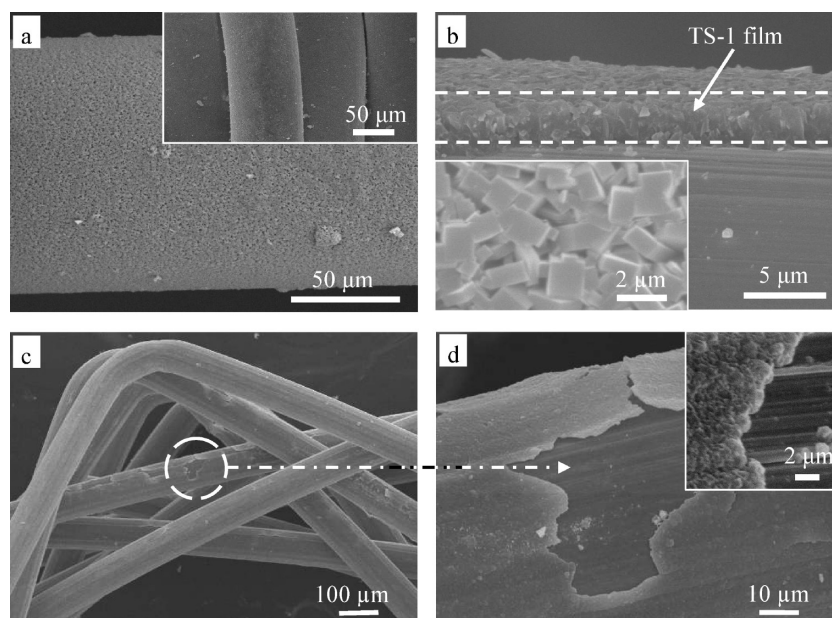


Figure 4. (a) SEM images of the TS-1 catalysts, (b) surface and cross-section of TS-1 films supported on stainless steel rings after calcinations in nitrogen protection, and (c, d) surface and cross section of TS-1 films supported on stainless steel rings after calcinations in air atmosphere.

Table 1. Catalytic Performance of the SSR Substrate, TS-1 Film and TS-1 Powder^a

catalyst	mass ^b (g)	Ti/Si ^c	Ti/Si ^c	X_{STY} (mol %)	conversion rate (R)	product selectivity (mol %)				H_2O_2 utilization	
						S_{AA}	S_{PAC}	S_{BAL}	S_{SO}	X (%)	$S_{\text{H}_2\text{O}_2}$ (%)
SSR	1.000			3.0	0.5	79.0	4.0	75.0	12.0		
TS-1 film (CP1)	0.077	0.014	0.015	12.0	25.6	91.0	67.0	24.0	5.0	50	73
TS-1 film (CP2)	0.080	0.018	0.019	16.0	32.8	99.1	90.1	9.0	0.4	55	90
TS-1 Powder (P1)	0.400	0.019 ^d	0.018	11.4	4.7	98.6	82.1	16.5	0.8	42	85
TS-1 powder (P2)	0.400	0.020 ^d	0.019	11.2	4.6	98.9	82.9	16.0	0.7	40	85

^a CP1, P1: calcinations in air atmosphere. CP2, P2: calcinations in nitrogen protection. R : millimoles of styrene converted per gram of catalyst per hour ($\text{mmol} \cdot \text{g}^{-1} \cdot \text{h}^{-1}$). X_{STY} : conversion of styrene. S_{AA} : sum of the selectivity of benzaldehyde (BAL) and phenylacetaldehyde (PAC). S_{PAC} , S_{BAL} , S_{SO} : selectivity of phenylacetaldehyde (PAC), benzaldehyde (BAL), and styrene epoxide. $S_{\text{H}_2\text{O}_2}$: mole percent H_2O_2 consumed in the formation of oxyfunctionalized product. ^b Net weight of TS-1. ^c Titanium content calculated by XPS. ^d Titanium content calculated by XRF. ^e Titanium content calculated by EDXS.

stainless steel ring displays the characteristic diffraction peaks of MFI zeolite at (011), (020), (051), (-303), (-313), and (-532) in the 2θ region between 5° and 30° , as shown in Figure 5b. Additional peaks found in the zeolite powder taken from the film coating also belong to MFI zeolites, confirming that the deposited zeolite was a pure MFI.

3.2. Titanium Species in TS-1-Coated Stainless Steel Packing Rings. The nature and amount of titanium in the calcined TS-1 film (CP2) were determined by FTIR, UV-vis, and XPS techniques. The FTIR and UV-vis were frequently used to characterize the titanium environment in the zeolites. The FTIR spectra of coated and uncoated stainless steel rings are shown in Figure 6a. The CP2 sample displayed a broad peak at 800 cm^{-1} assigned to symmetric Si-O-Si vibration in MFI,⁴⁴ whereas the 960 cm^{-1} band was interpreted to belong to the stretching vibration of SiO_4 units bound to titanium atoms and often taken to indicate the presence of framework titanium atom in TS-1.⁴⁵ The weak 960 cm^{-1} absorption band was due to the thinness of the zeolite coating, which was in agreement with previous reports.^{15,16}

The corresponding UV-vis spectra of the coated and uncoated samples are shown in Figure 6b. The broad absorbance peak at $\sim 210 \text{ nm}$ in the UV-vis spectrum of CP2 belongs to the tetrahedrally coordinated, framework titanium.⁴⁶ The characteristic signals of anatase TiO_2 at 330 nm and nanophase TiO_2 at 270 nm were not detected.⁴⁷ The CP1 catalyst shows absorbance at 330 nm for extraframework anatase TiO_2 in addition to 210 nm attributed to the framework titanium.

The deposited TS-1 was analyzed by XPS to determine the surface elemental composition and oxidation state of the sample.⁴⁸ The high resolution photoelectron spectra of O 1s and Ti $2p_{3/2}$ of TS-1 films from CP1 and CP2 samples are shown in Figure 7. Prior works by Uguina and co-workers⁴⁹ reported that tetrahedral titanium has a Ti $2p_{3/2}$ binding energy higher than 460 eV , whereas the lower binding energy component (458.5 eV) belongs to titanium in octahedral coordination. The O 1s binding energy of 533 eV shown in Figure 7a belongs to the oxygen from O-Si-O.⁵⁰ The XPS spectrum of the CP2 showed that the tetrahedral titanium species predominated in the

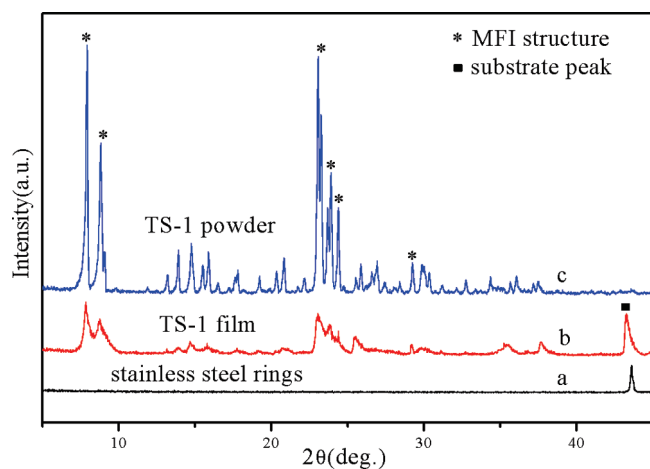


Figure 5. (a) XRD patterns of the stainless steel rings, (b) TS-1 film supported on stainless steel rings, and (c) TS-1 powder collected from the bottom of autoclave.

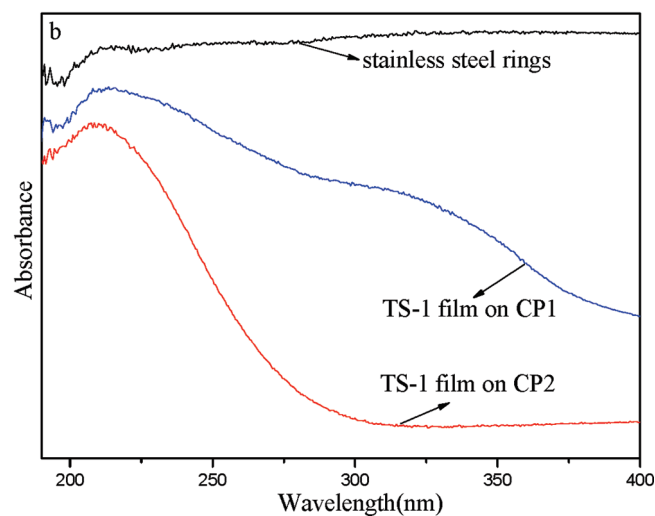
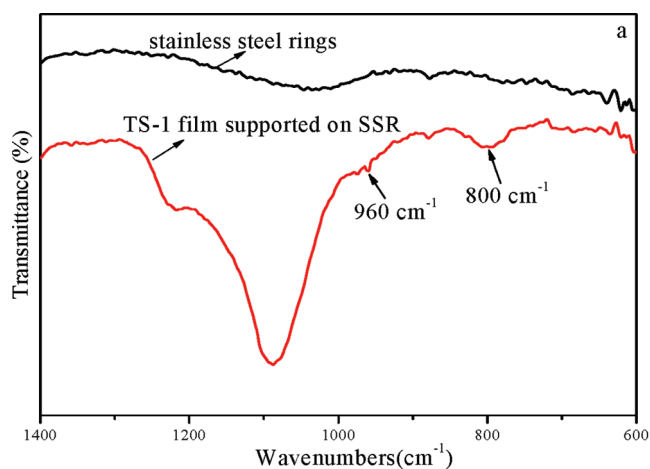


Figure 6. The FTIR (a) and UV-vis (b) spectra of stainless steel rings and TS-1 films supported on stainless steel rings calcined in air and nitrogen atmosphere.

deposited zeolite, which was in good agreement with the FTIR and UV-vis results shown in Figure 6a and b, respectively. XPS

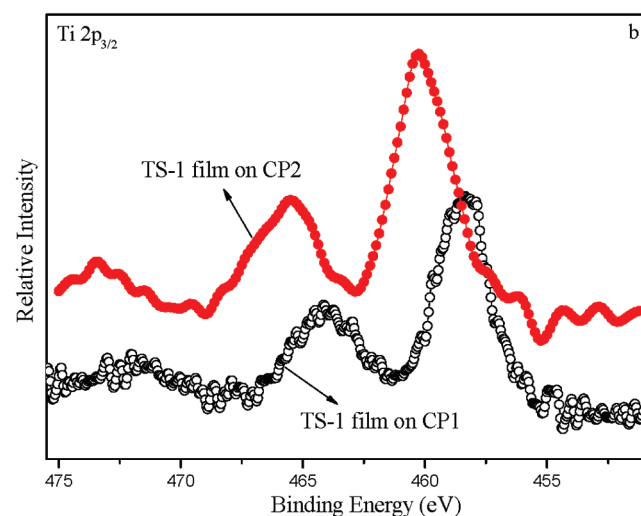
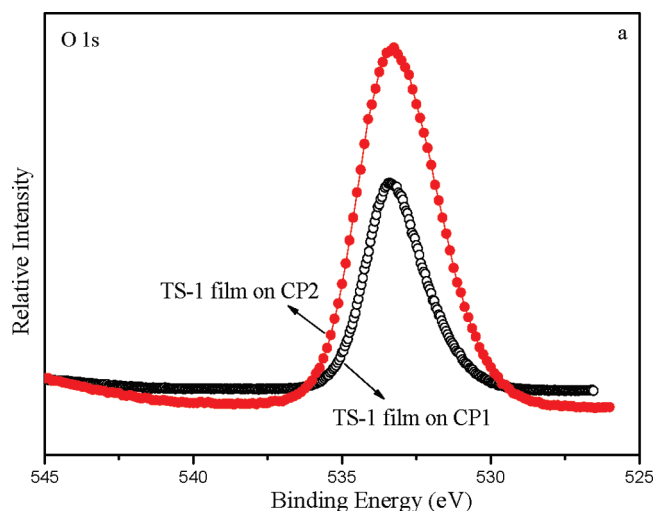
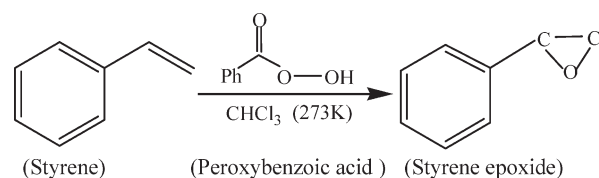


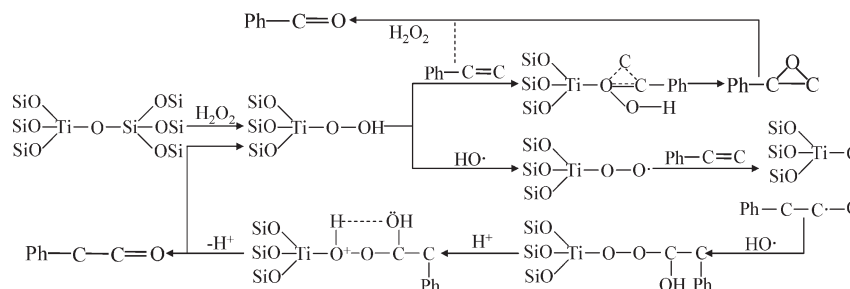
Figure 7. The O 1s (a) and Ti 2p_{3/2} (b) spectra of TS-1 films supported on stainless steel rings calcined in air and nitrogen atmosphere.

Scheme 1. Prilezhaev Reaction Scheme for Selective Oxidation of Styrene



spectra of CP1 in contrast showed mostly octahedral titaniums. Table 1 shows the Ti/Si ratios from XPS and EDXS are comparable and are close to the value of 0.02, indicating that most of the titanium supplied in the mother liquor was incorporated in the zeolites. This value is comparable to TS-1 zeolites prepared by conventional synthesis.^{3,51}

3.3. Catalytic Activity of TS-1-Coated Stainless Steel Packing Rings. The selective oxidation of styrene to styrene oxide is typically carried out using peroxybenzoic acid in Prilezhaev reaction (Scheme 1), whereas the TS-1-catalyzed reaction produces phenylacetaldehyde (PAC) and benzaldehyde (BAL), as shown in Scheme 2.⁵² Reaction data for the TS-1-coated packing

Scheme 2. Styrene Oxidation Reaction over TS-1 Catalysts According to Zhuang et al.⁵²Table 2. Catalytic Performance of This Work and Reported in Other Papers^a

catalyst	mass (g)	X_{STY} (%)	conversion rate (R)	TOF (h^{-1})	S_{PAC} (%)	S_{BAL} (%)	ref
powder	1	9.4			81.8	18.2	55
powder	0.2	35.4	2.95	5.9	74.2	22.8	56
powder	0.1	21.1	3.71	9.75	41.3	26.5	57
powder	0.416	56	2.24	1.1 ^b	44	29	58
powder	0.2	38.9	3.2	10.1	80.5	17.8	this work ^{b*}
film (CP1)	0.077	12.0	25.6	85.8	67.0	24.0	this work
film (CP2)	0.080	16.0	32.8	102.6	90.1	9.0	this work

^a X_{STY} = the conversion of styrene; S_{PAC} , S_{BAL} = the selectivity of phenylacetaldehyde (PAC) and benzaldehyde (BAL); R = mmol of styrene converted per gram catalyst per hour ($\text{mmol} \cdot \text{g}^{-1} \cdot \text{h}^{-1}$); TOF = moles of styrene converted per mole of Ti in the catalyst per hour. ^b Moles of H_2O_2 conversion for producing styrene oxide + secondary products per mole of Ti per hour. ^{b*} The reaction conditions are similar to ref 56.

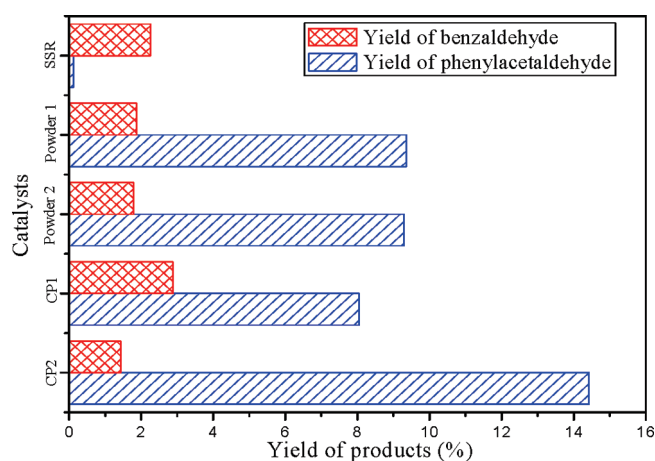


Figure 8. Benzaldehyde and phenylacetaldehyde yields on various catalysts (SSR, 1 g; CP1, 0.077 g TS-1; CP2, 0.08 g TS-1; P1, 0.4 g; and P2, 0.4 g).

rings (i.e., CP1 and CP2) as well as TS-1 powders collected from the same synthesis batch are summarized in Tables 1 and 2. The TS-1 powders calcined in air (P1) and pyrolyzed in nitrogen (P2) have comparable reaction performance (Table 1). The TS-1 powders displayed similar conversion of 11% and selectivity for phenylacetaldehyde of 82%. There was no significant difference in H_2O_2 conversion and H_2O_2 efficiency between the two powder catalysts, as shown in Table 1. TS-1-coated packing rings heat-treated in nitrogen (CP2) were better, with $\sim 40\%$ higher styrene conversion and better selectivity to phenylacetaldehyde, in addition to having higher H_2O_2 efficiency. An order of magnitude higher styrene conversion rate of coated TS-1 film

catalyst is attributed to the large interfacial contact area provided by stainless steel packing rings leading to improved mass transfer processes.¹⁰

A reference reaction carried out with uncoated stainless steel rings gave a low styrene conversion of $\sim 3\%$ with benzaldehyde as the main product ($Y_{\text{BAL}} = 2.25\%$) and trace phenylacetaldehyde ($Y_{\text{PAC}} = 0.12\%$), as shown in Table 1 and Figure 8. The styrene conversion and phenylacetaldehyde yield were higher for the TS-1-coated rings. TS-1-coated packing rings heat-treated in air (CP1) exhibited higher catalytic activity with styrene conversion and phenylacetaldehyde selectivity of 12% and 67%, respectively. Styrene conversion of 16% and phenylacetaldehyde selectivity of 90% were obtained from TS-1-coated packing rings pyrolyzed in nitrogen (CP2). Only a small amount of epoxide ($Y_{\text{SO}} = 0.06\%$) was produced by CP2 catalyst. It can be seen from the plots of phenylacetaldehyde and benzaldehyde yields in Figure 8 that the CP2 catalyst has the highest phenylacetaldehyde yield of 14.4%.

According to Zhuang and co-workers,⁵² the isolated titanium centers and Brønsted acid sites originating from framework titanium species favor phenylacetaldehyde production, whereas the Lewis acid, extra-framework titaniums catalyze the formation of benzaldehyde. Yang and co-workers⁵³ showed that extra-framework titanium species specifically catalyze the carbon-carbon bond cleavage that leads to the formation of benzaldehyde. The Lewis acid sites from iron could explain why benzaldehyde was the main product of styrene oxidation over the stainless steel rings. The TS-1-coated rings prepared by air calcination (CP1) displayed higher styrene conversion with conversion rate of $25.6 \text{ mmol} \cdot \text{g}^{-1} \cdot \text{h}^{-1}$. The CP1 catalyst also displayed higher phenylacetaldehyde yield than the uncoated ring, but the amount of benzaldehyde was still significant due to the presence of Lewis acid sites from naked SSR support and the

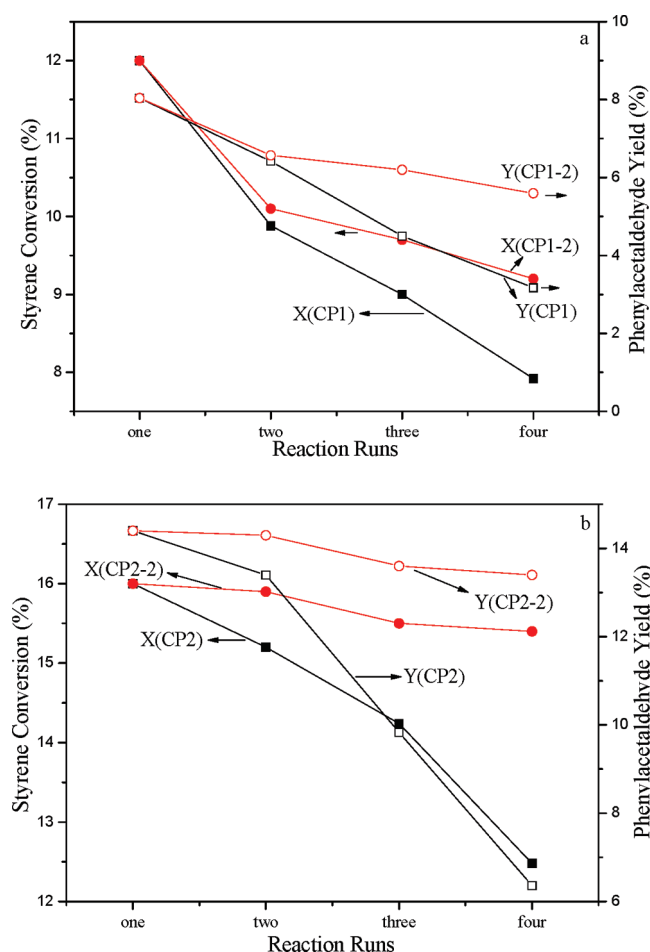


Figure 9. Reaction study of CP1 and CP2 catalyst (CP1 and CP2, treated by simple washing; CP1-2 and CP2-2, calcined in air).

extra-framework titanium species in this catalyst. The CP2 catalyst prepared by pyrolysis under nitrogen atmosphere displayed higher framework titanium content compared with the air calcined CP1 catalyst. The CP2 catalyst reached a styrene conversion and phenylacetaldehyde yield of 16% and 14.4%, respectively. This catalyst gave a conversion rate of $32.8 \text{ mmol} \cdot \text{g}^{-1} \cdot \text{h}^{-1}$, $\sim 30\%$ higher than the CP1 catalyst. Iron and extra-framework titanium are known to decompose H_2O_2 .⁵⁴ Indeed, CP1 catalyst has significantly lower H_2O_2 efficiency of 73% when compared with 90% obtained from CP2 catalyst. The H_2O_2 efficiency of CP2 catalyst is even higher than the powder catalyst P2 (85%), further proof of the improved mass transport processes on packing ring supported catalysts.

The TS-1 powder calcined in air (P1) recovered from the preparation TS-1-coated stainless steel rings displayed conversion and selectivity that was higher than literature reports (Table 2). A 0.2 g portion of powder catalyst gave a styrene conversion of 38.9% and conversion rate of $3.24 \text{ mmol} \cdot \text{g}^{-1} \cdot \text{h}^{-1}$ and TOF of 10.1 h^{-1} under reaction conditions comparable to the work of Kumar and co-workers.⁵⁶ The phenylacetaldehyde selectivity of 80.5% belonged to the upper range of reported values.^{55–58} The CP1 and CP2 catalysts have high conversion rates of 25.6 and $32.8 \text{ mmol} \cdot \text{g}^{-1} \cdot \text{h}^{-1}$ and corresponding TOFs of 85.8 and 102.6 h^{-1} . This represents nearly an order of magnitude enhancement in reaction rate from the powder catalyst recovered from the same batch of zeolites synthesis.

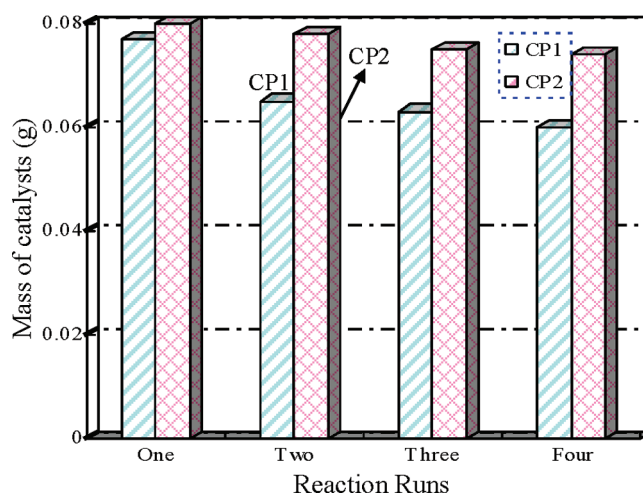


Figure 10. The mass of CP1 and CP2 catalysts (calcinations after each run) with reaction runs.

Table 3. Recycling of the TS-1-Coated Packing Rings Heat Treated in Nitrogen (CP2)^a

run	time (h)	X_{STY} (%)		initial TOF (h^{-1})		Ti/Si molar ratio ^d
		CP2 ^b	CP2-2 ^c	CP2	CP2-2	
1	1	6.0	6.0	193.0	193.0	0.019
2	1	5.6	5.8	185.2	191.9	0.019
3	1	4.5	5.5	155.1	189.6	0.018
4	1	2.7	5.4	94.3	188.5	0.016

^a X_{STY} = the conversion of styrene; TOF = moles of styrene converted per mole of Ti in the catalyst per hour. ^b Treated by simple washing with distilled water. ^c Treated by calcinations at 823 K after washing with distilled water. ^d The titanium content calculated by EDXS.

Although rapid mixing could disperse the powder catalyst well and facilitate the transport of the reactants to the catalyst surface, the external mass transfer through the liquid phase remained important.¹ The structured packing provides a large interfacial area and promotes mixing, resulting in higher external mass transfer rate. In addition, the thin catalyst layer has shorter diffusion pathways for the reactant and products. Prior works^{15,16} showed that the selective oxidation reaction occurred mostly on the top layer of the zeolite film and beyond a certain thickness the conversion remained unchanged. A combination of these factors is responsible for the observed high reaction rate of the TS-1-coated packing rings.

3.4. Deactivation and Regeneration of TS-1 Coated Stainless Steel Packing Rings. The deactivation and regeneration of TS-1 catalyst-coated packing rings, CP1 and CP2, were examined in a separate study.⁵⁹ The catalyst deactivation was observed in a series of four reaction runs each lasting 5 h. Reaction residues on the catalyst were removed by washing with distilled water after each run. The plots of styrene conversion and phenylacetaldehyde yield are shown in Figure 9a. The CP1 catalyst displayed rapid deactivation, with the conversion decreasing from 12 to 8%. Correspondingly, the phenylacetaldehyde yield decreased from 8 to 3.2%. In a parallel set of experimental study, air calcination at 823 K and 5 h was used to regenerate the spent CP1 catalyst.⁶⁰ The phenylacetaldehyde yield decreased with increasing number of runs due to the loss of catalyst, but the

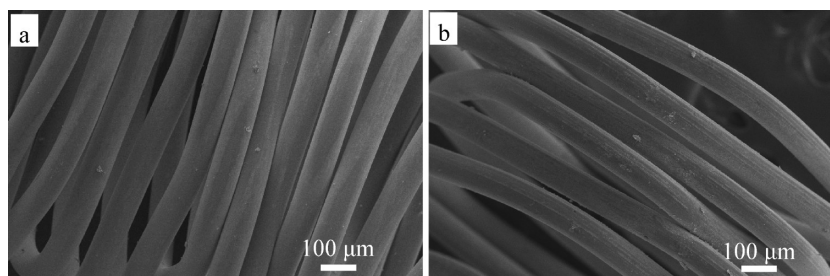


Figure 11. SEM images of the CP2 catalyst (a) before reaction and (b) after four reactions.

selectivity of phenylacetaldehyde remained unchanged after four reactions runs.

The plot of styrene conversion in Figure 9a shows that the catalyst could not be completely regenerated, and there is irreversible loss of catalyst activity after successive runs that appear to correlate well with the loss in catalyst mass observed in the CP1 catalyst (Figure 10). There is a nearly linear correlation between mass and catalyst activity loss for CP1 catalyst. It is speculated that the cracks and defects in CP1 catalyst caused by rapid removal of organic structure-directing agent (SDA) by air calcinations provide transport routes for oxygen to the support, resulting in oxidation at the support–zeolite interface, weakening the adhesion of the zeolite. This could explain the significant loss in catalyst mass and activity observed in Figures 9a and 10.

The TS-1-coated CP2 packing rings deactivate less than the CP1 catalyst, as seen in Figure 9b. The styrene conversion decreased from 16 to 12.5% after four reaction runs with ~22% drop in activity compared with 34% for the CP1 catalyst. The reaction results showed CP1 and CP2 catalysts suffered from deactivation caused by strongly adsorbed organic molecules. The selectivity of phenylacetaldehyde decreased from 90 to 51%, and the desired product phenylacetaldehyde yield reduced from 14.4 to 6.4%. The reaction data of CP1-2 and CP2-2 in Figure 9 represent the loss of activity due to loss in catalyst mass caused by delamination. Unlike CP1 catalyst, the original activity and selectivity of CP2 catalyst was fully recovered after calcination. Analysis of the CP2 catalyst after reaction showed that the catalyst Ti/Si ratio remained unchanged (Table 3), and the catalytic film remained firmly attached to that stainless steel surface, as shown in Figure 11. The zeolite coating on CP2 being more uniform and having less defects (cf. Figure 4a, b) is an efficient diffusion barrier for oxygen, limiting the corrosion of the stainless steel that could lead to film delamination. Indeed, many studies have showed that zeolite coatings were efficient corrosion-barrier and had proposed them as corrosion-resistant coatings.⁶¹

4. CONCLUSIONS

This work successfully demonstrated that catalyst-coated structured packing materials could significantly increase the reaction rate by improving transport processes. The structured packing materials are designed to provide large interfacial contact area while minimizing pressure drop in the reactor. The thin catalyst layer also affords short diffusion paths for reactants and products. Indeed, the TS-1-coated packing rings exhibited an order of magnitude higher conversion rate than the TS-1 powder prepared from the same batch of catalyst.

The use of organic linkers was instrumental in depositing a uniform seed layer for zeolite growth. Most of the titanium was

incorporated into the zeolite framework; however, pretreatment in air resulted in film deterioration and an increase in extra-framework titanium. TS-1 delamination was attributed to rapid zeolite contraction from the fast removal of the organic template molecules, resulting in crack formations. Heat treatment in nitrogen preserved the film structure as well as the framework titanium and led to a higher conversion rate and better phenylacetaldehyde selectivity. A significant increase in the reuse efficiency and a very high regenerability over the CP2 catalyst were achieved in comparison with the CP1 catalyst. The structured packing catalysts could be reused several times.

AUTHOR INFORMATION

Corresponding Author

*(X.F.Z.) Phone: +86 411 84986155. Fax: +86 411 84986155. E-mail: xfzhang@dlut.edu.cn. (J.S.Q.) Phone: +86 411 849866024. Fax: +86 411 84986024. E-mail: jqiu@dlut.edu.cn. (K.L.Y.) Phone: +852 2358 7123. Fax: +852 2358 0054. E-mail: kekyeung@ust.hk.

ACKNOWLEDGMENT

This work was partly supported by the National Natural Science Foundation of China (Grant No. 20673017, 21076030, 21036006), PetroChina Innovation Foundation (Grant No. 2008D-5006-05-06), Program for Liaoning Excellent Talents in University (Grant No. LR201008), and Universities Science & Research Project of Liaoning Province Education Department (Grant No. 2009S019). The authors also thank the Materials Characterization and Preparation Facility (MCPF) of the Hong Kong University of Science and Technology for the characterization of samples.

REFERENCES

- (1) Bhaumik, A.; Mukherjee, P.; Kumar, R. *J. Catal.* **1998**, *178*, 101–107.
- (2) Bianchi, D.; Bortolo, R.; Tassinari, R.; Ricci, M.; Vignola, R. *Angew. Chem., Int. Ed.* **2000**, *39*, 4321–4323.
- (3) Taramasso, M.; Perego, G.; Notari, B. U.S. Patent 4410501, 1983.
- (4) Notari, B. *Catal. Today* **1993**, *18*, 163–172.
- (5) Perego, C.; Carati, A.; Ingallina, P.; Mantegazza, M. A.; Bellussi, G. *Appl. Catal., A* **2001**, *221*, 63–72.
- (6) Li, G.; Wang, X. S.; Yan, H. S.; Liu, Y. H.; Liu, X. W. *Appl. Catal., A* **2002**, *236*, 1–7.
- (7) Serrano, D. P.; Sanz, R.; Pizarro, P.; Moreno, I.; de Frutos, P.; Blázquez, S. *Catal. Today* **2009**, *143*, 151–157.
- (8) Hu, C. W.; Zhu, L. F.; Xia, Y. S. *Ind. Eng. Chem. Res.* **2007**, *46*, 3443–3445.

- (9) Kotorá, M.; Svandová, Z.; Markos, J. *Chem. Pap.* **2009**, *63*, 197–204.
- (10) Dechaine, G. P.; Ng, F. T. T. *Ind. Eng. Chem. Res.* **2008**, *47*, 9304–9313.
- (11) Jung, K. T.; Shul, Y. G. *Chem. Mater.* **1997**, *9*, 420–422.
- (12) Lee, Y.; Ryu, W.; Kim, S. S.; Shul, Y.; Je, J. H.; Cho, G. *Langmuir* **2005**, *21*, 5651–5654.
- (13) Liu, Y.; Zong, L.; Xin, F. *Mater. Res. Innovations* **2008**, *12*, 84–89.
- (14) Au, L. T. Y.; Chau, J. L. H.; Ariso, C. T.; Yeung, K. L. *J. Membr. Sci.* **2001**, *183*, 269–291.
- (15) Qiu, F. R.; Wang, X. B.; Zhang, X. F.; Liu, H. O.; Liu, S. Q.; Yeung, K. L. *Chem. Eng. J.* **2009**, *147*, 316–322.
- (16) Wang, X. B.; Zhang, X. F.; Liu, H. O.; Yeung, K. L.; Wang, J. Q. *Chem. Eng. J.* **2010**, *156*, 562–570.
- (17) Wang, X. B.; Guo, Y.; Zhang, X. F.; Wang, Y.; Liu, H. O.; Wang, J. Q.; Qiu, J. S.; Yeung, K. L. *Catal. Today* **2010**, *156*, 288–294.
- (18) Cheng, Y. S.; Pena, M. A.; Fierro, J. L.; Hui, D. C. W.; Yeung, K. L. *J. Membr. Sci.* **2002**, *204*, 329–340.
- (19) Motuzas, J.; Mikutavičiūtė, R.; Gerardin, E.; Julbe, A. *Microporous Mesoporous Mater.* **2010**, *128*, 136–143.
- (20) Ke, X. B.; Zeng, C. F.; Yao, J. F.; Zhang, L. X.; Xu, N. P. *Mater. Lett.* **2008**, *62*, 3316–3318.
- (21) Zhao, Q.; Li, P.; Li, D. Q.; Zhou, X. G.; Yuan, W. K.; Hu, X. J. *Microporous Mesoporous Mater.* **2008**, *108*, 311–317.
- (22) Wan, Y. S. S.; Chau, J. L. H.; Gavriilidis, A.; Yeung, K. L. *Chem. Commun.* **2002**, 878–879.
- (23) Chau, J. L. H.; Wan, Y. S. S.; Gavriilidis, A.; Yeung, K. L. *Chem. Eng. J.* **2002**, *88*, 187–200.
- (24) Wan, Y. S. S.; Chau, J. L. H.; Yeung, K. L.; Gavriilidis, A. *J. Catal.* **2004**, *223*, 241–249.
- (25) Wan, Y. S. S.; Yeung, K. L.; Gavriilidis, A. *Appl. Catal., A* **2005**, *281*, 285–293.
- (26) Ha, K.; Lee, Y. J.; Lee, H. J.; Yoon, K. B. *Adv. Mater.* **2000**, *12*, 1114–1117.
- (27) Ha, K.; Park, J. S.; Oh, K. S.; Zhou, Y. S.; Chun, Y. S.; Lee, Y. J.; Yoon, K. B. *Microporous Mesoporous Mater.* **2004**, *72*, 91–98.
- (28) Chen, X. S.; Chen, P.; Kita, H. *Microporous Mesoporous Mater.* **2008**, *115*, 164–169.
- (29) Chau, J. L. H.; Leung, A. Y. L.; Yeung, K. L. *Lab Chip* **2003**, *3*, 53–55.
- (30) Sebastián, V.; Lin, Z.; Rocha, J.; Téllez, C.; Santamaría, J.; Coronas, J. *J. Membr. Sci.* **2008**, *323*, 207–212.
- (31) Zhang, X. F.; Liu, H. O.; Yeung, K. L. *Mater. Chem. Phys.* **2006**, *96*, 42–50.
- (32) Yeung, K. L.; Sebastian, J. M.; Varma, A. *Catal. Today* **1996**, *25*, 231–236.
- (33) Yeung, K. L.; Aravind, R.; Szegner, J.; Varma, A. *Stud. Surf. Sci. Catal.* **1996**, *101*, 1349–1358.
- (34) Maira, A. J.; Lau, W. N.; Lee, C. Y.; Yue, P. L.; Chan, C. K.; Yeung, K. L. *Chem. Eng. Sci.* **2003**, *58*, 959–962.
- (35) Yeung, K. L.; Zhang, X. F.; Lau, W. N.; Martin-Aranda, R. *Catal. Today* **2005**, *110*, 26–37.
- (36) Yang, G. H.; Zhang, X. F.; Liu, S. Q.; Yeung, K. L.; Wang, J. Q. *J. Phys. Chem. Solids* **2007**, *68*, 26–31.
- (37) Chau, J. L. H.; Tellez, C.; Yeung, K. L.; Ho, K. *J. Membr. Sci.* **2000**, *164*, 257–275.
- (38) Au, L. T. Y.; Yeung, K. L. *J. Membr. Sci.* **2001**, *194*, 33–55.
- (39) Lai, S. M.; Au, L. T. Y.; Yeung, K. L. *Microporous Mesoporous Mater.* **2002**, *54*, 63–77.
- (40) Heng, S.; Lau, P. P. S.; Yeung, K. L.; Djafer, M.; Schrotter, J. C. *J. Membr. Sci.* **2004**, *243*, 69–78.
- (41) Motuzas, J.; Heng, S.; Lau, P. P. S.; Yeung, K. L.; Beresnevicius, Z. J.; Julbe, A. *Microporous Mesoporous Mater.* **2007**, *99*, 197–205.
- (42) Heng, S.; Yeung, K. L.; Djafer, M.; Schrotter, J. C. *J. Membr. Sci.* **2007**, *289*, 67–75.
- (43) Fejes, P.; Nagy, J. B.; Halász, J.; Oszkó, A. *Appl. Catal., A* **1998**, *175*, 89–104.
- (44) Drago, R. S.; Dias, S. C.; McGilvray, J. M.; Mateus, A. L. M. L. *J. Phys. Chem. B* **1998**, *102*, 1508–1514.
- (45) Uguina, M. A.; Serrano, D. P.; Ovejero, G.; Van Grieken, R.; Camacho, M. *Appl. Catal., A* **1995**, *124*, 391–408.
- (46) Klein, S.; Weckhuysen, B. M.; Martens, J. A.; Maier, W. F.; Jacobs, P. A. *J. Catal.* **1996**, *163*, 489–491.
- (47) Mantegazza, M. A.; Petrini, G.; Spanò, G.; Bagatin, R.; Rivetti, F. *J. Mol. Catal. A: Chem.* **1999**, *146*, 223–228.
- (48) Reddy, J. S.; Sayari, A. *Stud. Surf. Sci. Catal.* **1995**, *94*, 309–316.
- (49) Uguina, M. A.; Serrano, D. P.; Sanz, R.; Fierro, J. L. G.; López-Granados, M.; Mariscal, R. *Catal. Today* **2000**, *61*, 263–270.
- (50) Davis, R. J.; Liu, Z. F. *Chem. Mater.* **1997**, *9*, 2311–2324.
- (51) Li, Y. G.; Lee, Y. M.; Porter, J. F. *J. Mater. Sci.* **2002**, *37*, 1959–1965.
- (52) Zhuang, J. Q.; Yang, G.; Ma, D.; Lan, X. J.; Liu, X. M.; Han, X. W.; Bao, X. H.; Mueller, U. *Angew. Chem., Int. Ed.* **2004**, *43*, 6377–6381.
- (53) Yang, Q. H.; Li, C.; Yuan, S. D.; Li, J.; Ying, P. L.; Xin, Q.; Shi, W. D. *J. Catal.* **1999**, *183*, 128–130.
- (54) Huybrechts, D. R. C.; Buskens, P. L.; Jacobs, P. A. *J. Mol. Catal.* **1992**, *71*, 129–147.
- (55) Zhuang, J. Q.; Ma, D.; Yan, Z. M.; Liu, X. M.; Han, X. W.; Bao, X. H.; Zhang, Y. H.; Guo, X. W.; Wang, X. S. *Appl. Catal., A* **2004**, *258*, 1–6.
- (56) Kumar, S. B.; Mirajkar, S. P.; Pais, G. C. G.; Kumar, P. *J. Catal.* **1995**, *156*, 163–166.
- (57) Hulea, V.; Dumitriu, E. *Appl. Catal., A* **2004**, *277*, 99–106.
- (58) Laha, S. C.; Kumar, R. *J. Catal.* **2001**, *204*, 64–70.
- (59) Jones, C. W. *Top. Catal.* **2010**, *53*, 942–952.
- (60) Wang, Q. F.; Wang, L.; Chen, J. X.; Wu, Y. L.; Mi, Z. T. *J. Mol. Catal. A: Chem.* **2007**, *273*, 73–80.
- (61) Lew, C. M.; Cai, R.; Yan, Y. S. *Acc. Chem. Res.* **2010**, *43*, 210–219.